Pollutant Dispersion and Bimodality in Tall Building Clusters

Dianfang Bi[1], Abhishek Mishra[1], Marco Placidi[1], Alan Robins[1], Matteo Carpentieri[1*]
[1]Environmental Flow Laboratory (EnFlo), School of Mechanical Engineering Sciences, University of Surrey
Guildford, Surrey, GU2 7XH, UK
[*] E-mail: m.carpentieri@surrey.ac.uk

1 INTRODUCTION

While tall buildings (TBs) are essential for sustainable city planning and efficient space management [1, 2], they also pose significant challenges regarding the dispersion of harmful pollutants from various sources, such as industrial sites and residential areas [3]. The interaction between the TB cluster and atmospheric boundary layers creates varied dispersion characteristics, which are not yet fully understood [4].

Investigations into the effects of single wall-mounted cylinders, representing individual buildings, have demonstrated the significant impact of shape on aerodynamic and pollutant dispersion characteristics [5, 6]. These studies reveal that TBs considerably influence flow and dispersion, enhancing vertical and lateral plume movement [7]. In homogeneous low-rise building arrays, plume dispersion retains a Gaussian form laterally and a reflected Gaussian form vertically, influenced by building geometry and atmospheric conditions [8].

In real urban settings, non-uniform canopies create complex roughness sublayers that significantly alter airflow and pollutant dispersion [9]. Research on TB clusters as 2D or 3D bluff bodies has focused on aerodynamic characteristics, wake formation, and the phenomenon of bleeding, which affects drag and wake dynamics [10]. As the solidity ratio of the TB cluster increases, wake formations elongate, canopy height increases and both advective and turbulent vertical scalar transport are enhanced.

A previous study by our group investigated wake flow behind varying building clusters, revealing distinct wake characteristics in near-, transition-, and far-wake regimes [11]. This paper extends that work by focusing on how building width W_B influences dispersion characteristics. Section 2 details the experimental setup, Section 3 presents the results, and Section 4 concludes the paper.

2 EXPERIMENT SETUP

The experiment was conducted in the EnFlo wind tunnel at the University of Surrey, with a working section of 20 meters in length, 1.5 meters in height, and 3.5 meters in width. To simulate the atmospheric boundary layer, Irwin spires were placed at the tunnel entrance, creating a boundary layer thickness of 1 meter. The tunnel floor featured a 50% staggered array of rectangular roughness elements to mimic urban conditions.

Building cluster models consisted of wooden cylinders with square cross-sections, each 60 mm wide (W_B) and 240 mm high (H_B), giving an aspect ratio (AR) of 4. The spacing between buildings (W_S) was set at $0.5W_B$, $1W_B$, and $3W_B$, all centrally positioned on a circular turntable 14 meters from the tunnel inlet. Velocity measurements were taken using a three-component Laser Doppler Anemometry (LDA) system with laser wavelengths of 532 nm, 552 nm, and 561 nm. The flow was seeded with sugar particles averaging 1 μm in diameter. Measurement duration at each point was 60 seconds, with a minimum acquisition frequency of 100 Hz. The free stream velocity was 2 m/s, measured by a sonic anemometer located 5 meters from the inlet. For dispersion experiments, propane was released from a ground-level circular source at the cluster centre. Concentrations were measured using a fast-response Flame Ionization Detector (FFID) positioned 5 mm downstream of the LDA measurement volume. Concentrations were sampled at 1000 Hz and averaged over 60 seconds, maintaining standard errors below 5% for mean values and below 10% for variance values.

DOI 10.5258/WES/P0055

3 RESULTS

Building spacing significantly influences plume development from a ground-level source at the cluster centre, as illustrated by the lateral mean concentration profiles at the mid-height of the building cluster ($z/H_B = 0.5$) in Figure 1. The concentration is non-dimensionalized by $\overline{c^*} = \bar{c}U_{ref}H_B^2/Q$, where U_{ref} is the reference velocity (freestream velocity measured by the sonic anemometer) and Q is the volumetric flow rate of the tracer gas.

Flow regions, near-, transition-, and far-wake, are classified based on the impacts of individual buildings as identified in [11]. In the near-wake region, separate wakes form immediately behind the cluster, from the trailing edge to $W_A < 0.45$ (where W_A is the cluster width), and merge into a single wake in the transition region ($0.45 < W_A < 1.5$). In the far-wake region ($W_A > 1.5$), a large cluster wake forms, similar to that behind a single isolated building. Figures 1 illustrate the different dispersion behaviours observed in these regions. Coordinates are normalized by the building width W_B to facilitate comparison across different cluster sizes.

Dispersion characteristics vary across flow regions, with notable bimodality in the near-wake regions for different building spacings, as shown in Figure 1. Further downstream, bimodality transitions to unimodality beyond the transition-wake region. Unimodal profiles in the transition and far-wake regions show similar trends but with decreasing concentration magnitude and wider spread. Notably, the peak value of the mean concentration profile in the near-wake region exceeds those in the transition- and far-wake regions, potentially exacerbating air quality issues at higher elevations.

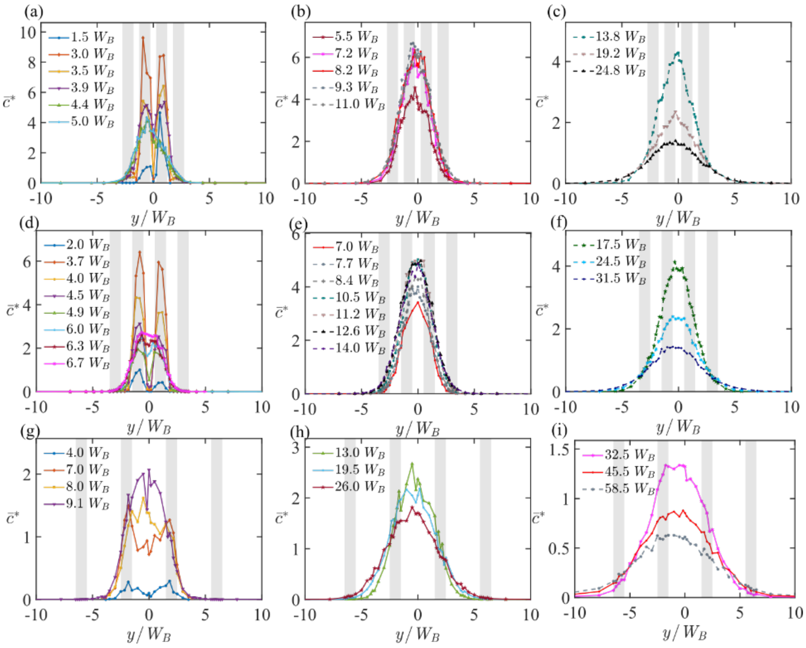

Figure 1, Lateral profiles of the mean concentration at $z/H_B = 0.5$ with three different building spacings: $W_S = 0.5W_B$ (subfigures (a) to (c)), $W_S = 1W_B$ (subfigures (d) to (f)) and $W_S = 3W_B$ (subfigures (g) to (i)). The shaded areas indicate the locations of the buildings

A non-parametric statistical approach, Hartigan's dip test [12], was used to analyse the multimodal characteristics of concentration profiles quantitatively. Due to the limited resolution of the original data, which were measured at discrete locations, a $20\times$ interpolation was applied, introducing 20 times the number of original data points between existing ones. Figure 2 shows the results of Hartigan's dip test of the different lateral concentration profiles along the streamwise direction at both the one-quarter and half height of the building cluster. Large dip values, indicating bimodality, are primarily observed in the near-wake region for clusters with small spacings ($W_S = 0.5W_B$ and $W_S = 1W_B$) at both $z/H_B = 0.25$ and $z/H_B = 0.5$. These dip values decline rapidly beyond the near-wake region, with only minor fluctuations and low values observed further downstream. For the wide spacing ($W_S = 3W_B$), the dip values approach zero for all streamwise locations at $z/H_B = 0.25$, with only small fluctuations observed at the mid-height of the cluster in the near- and transition-wake regions.

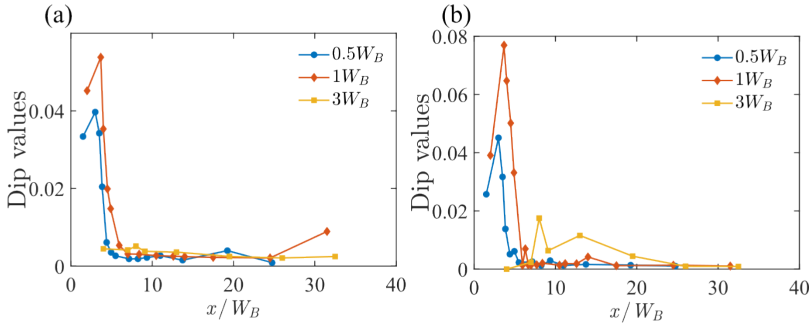

Figure 2, Hartigans' dip values at $z/H_B = 0.25$ and $z/H_B = 0.5$ for the three different building spacings.

To better quantify the effects of spacing on the plume depth, we applied Gaussian distribution fitting to the vertical profiles to determine plume boundaries. The plume boundary at each streamwise position was defined to enclose 90% of the total tracer particles, calculated by integrating the area under the fitted Gaussian curves:

$$90\% = \frac{\int_0^{y_u^*} \bar{c}^* dy^*}{\int_{-\infty}^{+\infty} \bar{c}^* dy^*} \tag{1}$$

where the denominator is the total pollutant tracer under the profile curve, and the numerator is the area enclosed by the upper boundaries y_u^*. Figure 3 shows that with increasing building width, the height of the plume in the far downstream decreases and approaches the plume development observed without any buildings. This indicates that the influence of the building cluster on the plume diminishes with wider spacing. Conversely, for the small spacing ($W_S = 0.5W_B$), the plume is lifted immediately after the cluster.

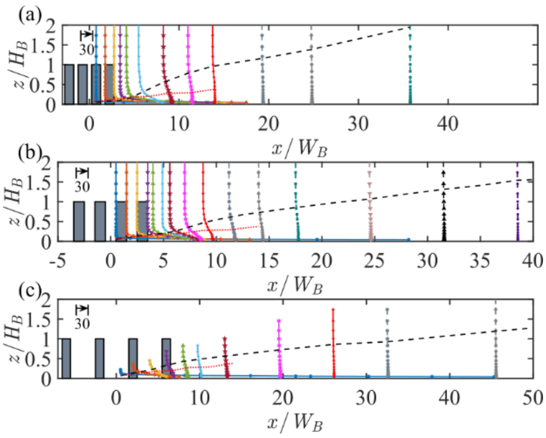

Figure 3, The vertical concentration profiles and the plume's vertical boundaries: (a) $W_S = 0.5W_B$; (b) $W_S = 1W_B$; (c) $W_S = 3W_B$. In each subfigure, the concentration profiles are shifted to the positions where they were measured, and the values are scaled down to 30 times the original values, for better visualization due to the relatively large values near the ground, especially for the measurement points near the source. The scaling magnitude is indicated by the arrow in the top left corner. The black dashed line represents the vertical boundary, and the red dotted line represents the results from an empty tunnel with no buildings for comparison.

In the vertical direction, Figure 4 displays the profiles of advective scalar flux ($\bar{w}\bar{c}^*$) and turbulent scalar flux ($\overline{wc}^*$) in the centre of the wake. For the narrow building spacing ($W_S = 0.5W_B$), $\bar{w}\bar{c}^*$ and $\overline{wc}^*$ have comparable magnitudes. As the building spacing increases, $\bar{w}\bar{c}^*$ decreases and even presents negative values for the cluster with $W_S = 3W_B$. This indicates that in denser clusters, pollutant particles are transported upward from the ground, resulting in higher pollutant levels at greater altitudes and a thicker plume depth. On the other hand, for the turbulent scalar flux ($\overline{wc}^*$), the maximum height of $\bar{w}\bar{c}^*$occurs near the canopy height and gradually decreases with wider building spacing.

DOI 10.5258/WES/P0055

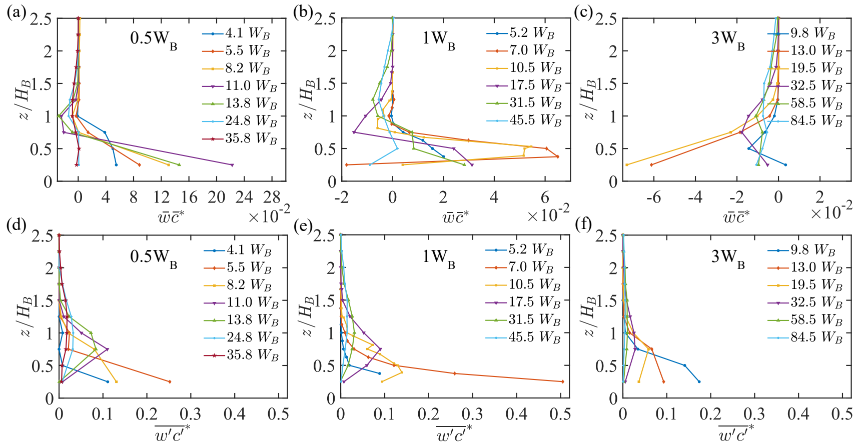

Figure 4, The vertical profiles of advective scalar flux $\overline{w}\bar{c}^*$and turbulent scalar flux $\overline{wc}^*$ along the centreline of the building cluster.

4 CONCLUSIONS

This study investigates the influence of building spacing (W_S) on pollutant dispersion within tall building clusters. The results show that building spacing significantly impacts plume development and dispersion characteristics. Narrow building spacings ($W_S = 0.5W_B$) enhance vertical plume movement, resulting in higher pollutant levels at greater altitudes and thicker plume depths. In contrast, wider spacings ($W_S = 3W_B$) diminish these effects, leading to a more uniform plume development akin to scenarios without buildings. The use of Hartigan's dip test and Gaussian fitting effectively quantified the bimodality and plume boundaries, revealing that the dispersion complexity decreases with increased building spacing. These findings underscore the critical role of building configuration in urban pollutant dispersion and provide valuable insights for urban planning and air quality management.

REFERENCES

[1] T.R. Oke, G. M. A. C. and J. A. Voo. (2018). Urban Climates. Cambridge University Press.

[2] Brunekreef, B., Holgate, S.T., 2002. Air pollution and health. The lancet 360, 1233–1242.

[3] Cassiani, M., Bertagni, M.B., Marro, M., Salizzoni, P., 2020. Concentration fluctuations from localized atmospheric releases. Boundary-Layer Meteorology 177, 461–510.

[4] Britter, R.E., Hanna, S.R., 2003. Flow and dispersion in urban areas. Annual Review of Fluid Mechanics 35, 469–496.

[5] Wang, H.F., Zhou, Y., Chan, C.K., Lam, K.S., 2006. Effect of initial conditions on interaction between a boundary layer and a wall-mounted finite-length-cylinder wake. Physics of Fluids 18.

[6] Behera, S., Saha, A.K., 2019. Characteristics of the flow past a wall-mounted finite-length square cylinder at low reynolds number with varying boundary layer thickness. Journal of Fluids Engineering 141, 061204.

[7] Heist, D.K., Brixey, L.A., Richmond-Bryant, J., Bowker, G.E., Perry, S.G., Wiener, R.W., 2009. The effect of a tall tower on flow and dispersion through a model urban neighborhood: Part 1. flow characteristics. Journal of Environmental Monitoring 11, 2163–2170.

[8] Marucci, D., Carpentieri, M., 2020. Dispersion in an array of buildings in stable and convective atmospheric conditions. Atmospheric Environment 222.

[9] Wang, L., Li, D., Gao, Z., Sun, T., Guo, X., Bou-Zeid, E., 2014. Turbulent transport of momentum and scalars above an urban canopy. Boundary-Layer Meteorology 150, 485–511.

[10] Wangsawijaya, D.D., Nicolai, C., Ganapathisubramani, B., 2023. Scalar transport in flow past finite circular patches of tall roughness. International Journal of Heat and Fluid Flow 102, 109167.

[11] Mishra, A., Placidi, M., Carpentieri, M., & Robins, A. (2023). Wake Characterization of Building Clusters Immersed in Deep Boundary Layers. Boundary-Layer Meteorology, 189(1), 163-187.

[12] Hartigan, J.A., Hartigan, P.M., 1985. The dip test of unimodality. The Annals of Statistics 13, 70–84.

DOI 10.5258/WES/P0055